RSC Advances

PAPER

View Article Online
View Journal | View Issue

Cite this: RSC Adv., 2015, 5, 25959

Study on key step of 1,3-butadiene formation from ethanol on MgO/SiO_2

Minhua Zhang,[ab] Meixiang Gao,[ab] Jianyue Chen[ab] and Yingzhe Yu*[ab]

Received 26th December 2014
Accepted 17th February 2015

DOI: 10.1039/c4ra17070a

www.rsc.org/advances

The structure and surface properties of the MgO/SiO_2 catalyst were studied by both experimental characterization and the simulation method. The adsorption properties of ethanol on different MgO/SiO_2 surfaces were researched by the density functional theory method and the result is that ethanol mainly adsorbed on MgO surface. The role of SiO_2 in increasing the MgO crystal defects in the MgO/SiO_2 has been obtained and the electronic properties of ethanol molecule before and after adsorption on the catalyst surfaces were compared. The initial step of ethanol dehydrogenation and the dehydration to 1,3-butadiene process, which is the dehydrogenation of ethanol to acetaldehyde reaction, on the flat sites, stepped sites and kinked sites was examined through the molecular simulation method. We investigated the preferable surface for the reaction of ethanol dissociation to an ethoxy group and the more active surface for the reaction of dehydrogenation of ethanol to acetaldehyde. The research results suggested that the stepped MgO surface is more active for the reaction of dehydrogenation of ethanol to acetaldehyde.

1 Introduction

1,3-Butadiene (BD) is one of the most essential basic chemicals in the petroleum chemical industry. BD is a by-product of the ethylene process typically isolated from the cracking of naphtha.[1] The recent trends in lightening of the feedstock of steam crackers reduce the BD supply and may potentially lead to a shortage in BD production in the coming years.[2] An estimated 9.3 million tons of BD were produced worldwide in 2005 (CMAI, 2006). The world capacity grew by 3.5% per year between 1997 and 2002.[3] To accommodate this up-coming energy deficit, it is especially crucial to develop alternative technologies for BD production from renewable resources such as bioethanol. Recent research has shifted toward bioethanol production from non-food biomass feedstocks.[4–6] Therefore, in the coming number of years, BD production from bioethanol will be the most promising, renewable and sustainable technology among various on-purpose BD production processes.

Catalytic BD formation from ethanol is an industrially proven route. From the 1920s to 1960s, ethanol was converted to BD at 400–450 °C using a one-step process or at 300–350 °C according to a two-step process using a Ta_2O_5/SiO_2 catalyst. Additionally, various catalysts have been proposed to perform this reaction.[7–11] Among all the catalysts that were suggested to catalyze this reaction, MgO/SiO_2 is the most widely studied, and Makshina *et al.*[12] also report that MgO/SiO_2 is the most promising catalyst in the reaction to transform ethanol to BD. However, the mechanism of the high MgO/SiO_2 activity achieved and the roles that SiO_2 play in the catalysis of MgO/SiO_2 are today open for debate. The reaction mechanism suggested by Lebedev *et al.*,[13] which is discussed in ref. 14, may be represented as follows:

$$(1)\ CH_3CH_2OH \rightarrow CH_3CHO + H_2\uparrow$$

$$(2)\ 2CH_3CHO \rightarrow CH_3CHOHCH_2CHO$$

$$(3)\ CH_3CHOHCH_2CHO \rightarrow CH_3{-}CH{=}CH{-}CHO + H_2O$$

$$(4)\ CH_3{-}CH{=}CH{-}CHO + CH_3CH_2OH \rightarrow CH_3CH{=}CHCH_2OH + CH_3CHO$$

$$(5)\ CH_3CH{=}CHCH_2OH \rightarrow CH_2{=}CH{-}CH{=}CH_2 + H_2O$$

In our previous work, we studied the reaction of MgO/SiO_2- and the mechanism of the catalytic conversion of ethanol to 1,3-butadiene on magnesia–silica acidic–basic bifunctional catalysts,[15,16] which agrees with the research by Lebedev *et al.*[13] The research by Branda *et al.*[17] shows that the catalytic activity of the MgO surfaces is attributed to its crystal defects, but no one accounts for the principle of ethanol conversion to BD on a defective MgO structure.

The aim of our present work is to apply a simulation method to study the key steps of BD formation from ethanol on MgO and SiO_2, to analyze the roles that SiO_2 play in the catalysis and the different characters of the defective surface of MgO, which

[a]Key Laboratory for Green Chemical Technology of Ministry of Education, Tianjin University R&D Center for Petrochemical Technology, Tianjin 300072, China. E-mail: yzhyu@tju.edu.cn

[b]Collaborative Innovation Center of Chemical Science and Engineering (Tianjin), Tianjin 300072, China

makes contributions to the research of BD formation on MgO/SiO_2 at the molecular level.

2 Experimental and computational methods

2.1 Preparation of the catalysts

The preparation method of wet-kneading was employed. The MgO content of the MgO/SiO_2 catalyst, the calcined temperature and favorable reaction conditions have been studied. When the MgO content was 80 wt%, the catalyst had the highest selectivity as listed in Table 1.[15,16]

2.2 Catalyst characterization

The solid structure in MgO, SiO_2 and MgO/SiO_2 samples were determined by powder X-ray diffraction methods using a D/max-2500 diffractometer and Ni-filtered CuKα radiation. The UV reflectance spectra of powdered samples were measured on a U-3010 UV-Vis DRS spectrophotometer.

2.3 Temperature-programmed surface reaction

The temperature-programmed surface reaction experiments were carried out in Auto II 2920 and products were analyzed by an on-line mass spectrometer (Balzers Omnistar MS200). The 100 mg MgO or SiO_2 (bought from Aladdin) was fixed in a quartz reactor. Before the experiment, the sample was pretreated in N_2 at 500 °C for 2 h at a heating rate of 20 °C min^{-1} from ambient temperature to 500 °C, and a N_2 flow rate of 20 ml min^{-1}. After the catalyst pretreated and the temperature drop to 400 °C, ethanol/He gas was injected to the catalyst surface through a quantitative loop (1 μl). The MS was used to detect all possible products: acetaldehyde, ethylene, and 1-butylene.

2.4 Computational methodology

The calculations were performed by the density functional theory program Dmol^3 in Materials Studio of Accelrys, in which the physical wave functions are expanded in the terms of numerical basis sets.[18,19] To maintain the balance between the efficiency and computation accuracy, a DNP double numerical basis set was used, and special points sampling integration were employed, a 2 × 2 × 1 *k*-point grid was determined by the Monkhorst–Pack method.[20] The core electrons were treated with DFT semi-core pseudopotentials.[21] The exchange–correlation energy was calculated using the Rectified-Perdew–Burke–Ernzerhof (RPBE) generalized gradient approximation (GGA).[22] The electron density and a self-consistent field tolerance were converged to within 2.0 × 10^{-5} eV and 1.0 × 10^{-5} Ha per atom, respectively. The geometry optimizations were performed with DFT until the force on each atom was less than 0.004 Ha $Å^{-1}$.

Table 1 Influence of different MgO content on the catalytic performance[16]

MgO content	$X_{ethanol}$%	S_{BD}%	$S_{ethylene}$%	$S_{diethyl\ ether}$%	$S_{acetic\ acid}$%
30%	66.90	15.08	73.39	10.53	1.77
40%	68.74	21.79	73.41	4.01	0.89
50%	63.90	26.80	69.16	3.31	0.71
70%	63.32	30.67	65.84	2.99	0.46
80%	66.32	48.02	49.08	2.15	0.74
90%	41.76	19.48	63.03	1.41	16.03

3 Results and discussion

3.1 Characterizations of MgO, SiO_2 and MgO/SiO_2

3.1.1 Crystallographic characterization. X-ray diffraction patterns of the samples showed typical diffractograms of MgO/SiO_2, Fig. 1, with peaks at 36.6°, 42.8°, 62.3° and 78.6°, which correspond to diffraction by the MgO planes (111), (200), (220) and (222), respectively. The phase is unambiguously identified according to the peaks at 20° to 30°, which corresponds to amorphous SiO_2. However, phases corresponding to $MgSiO_4$ were not detected in the MgO/SiO_2 catalyst. The X-ray analyses show that MgO and SiO_2 still maintain their native morphology in the MgO/SiO_2, and compared with MgO, sample MgO/SiO_2 presents peaks wider and less intense.

3.1.2 Coordination characterization. The UV diffuse reflectance spectra of MgO/SiO_2 and MgO are presented in Fig. 2. The catalyst MgO/SiO_2, in addition to an intense peak at 230 nm, shows a second peak at 275 nm. The MgO shows a peak at 235 nm and a weak shoulder around 320 nm. Coluccia *et al.*[23,24] have observed peaks at 230 and 274 nm from a study of several MgO samples, which they associated with four-coordinate, and three-coordinate O^{2-} ions, respectively. Thus, we can make the conclusion that for the catalyst MgO/SiO_2, the addition of SiO_2 would lead to structural modifications in the MgO such as an increase in the flat, stepped and kinked defects and in the coordinatively unsaturated O^{2-} ions and Mg–O–Si interactions, which provides a basis for establishing the model.

3.2 The surface reaction of ethanol on MgO and SiO_2

The ion intensity of products against the reaction time on the MgO and SiO_2 surface, with ethanol pulse injection, are shown

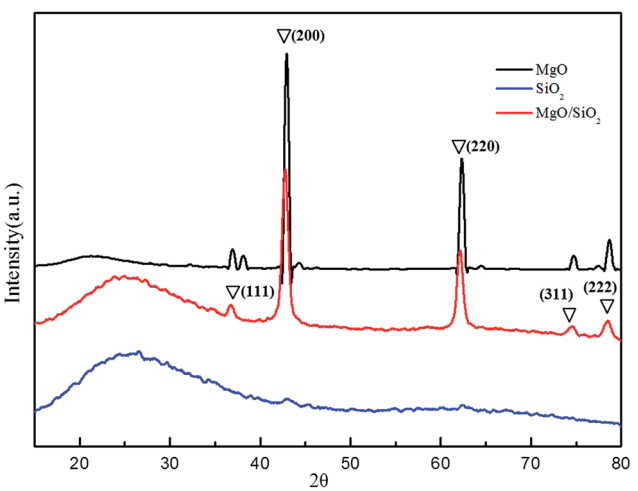

Fig. 1 XRD patterns for MgO/SiO_2, MgO and SiO_2 catalyst.

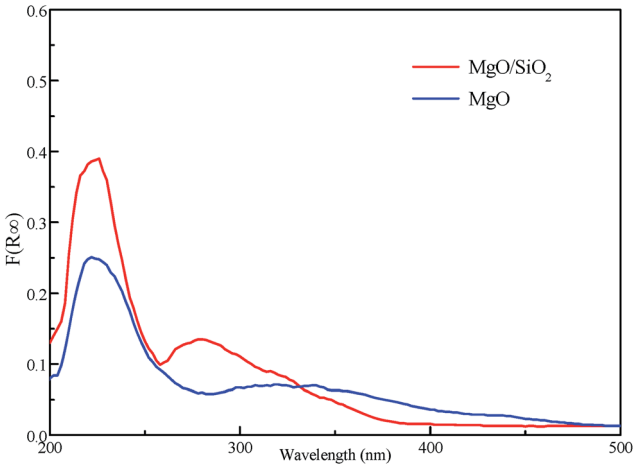

Fig. 2 UV diffuse reflectance spectra of MgO/SiO_2 catalyst and MgO catalyst samples.

in Fig. 3 and 4. The products are acetaldehyde, ethylene and 1-butene on the MgO surface, while only ethylene is formed from ethanol on the SiO_2 surface. Further, we can speculate that the effect of ethanol on MgO: ethylene is formed from ethanol through dehydration; ethanol is dehydrogenated to acetaldehyde; acetaldehyde underwent an aldol-condensation with reduction and dehydration forming 1-butene. Similarly, the process of ethanol on SiO_2 is dehydration of ethanol to ethylene. Based on the process of formation of BD from ethanol listed in the literature,[2,8,12] the first and key step is dehydrogenation of ethanol to acetaldehyde. Thus, the study of the key step of the formation of BD from ethanol at molecular level is a priority.

3.3 Models

As above, experimental research shows that the MgO and SiO_2 still maintain their native morphology in MgO/SiO_2 and phases corresponding to $MgSiO_4$ are not detected. Thus, we model MgO and SiO_2, respectively. The partial structure of amorphous silica is similar to β-cristobalite; furthermore, the physical properties such as the density, refractive index are found to be close. Thus, we selected β-cristobalite with *Fd*3*m* symmetries as the representative model of silica,[25,26] as shown in Fig. 5. The lattice constant $a = b = c = 7.16$ Å agrees satisfactorily with experimental measurements.[27] The results of the experiment show that the surface hydroxyls density of amorphous silica is 4.9 OH/100 $Å^2$,[28] while that of β-cristobalite (111) is 4.55 OH/100 $Å^2$. The supercell for the (111) surface include a (2×2) surface unit cell and 4 atomic layers with a vacuum region of 15 Å, and maintain the other two layers of the slab fixed in the geometry.

Avoiding unphysical dipole–dipole interactions between two consecutive slabs, we adopted an asymmetry supercell in which the atoms of the uppermost layer were satisfied by OH and the bottom Si atoms were unsatisfied.

The alkalinity of metal oxide mainly lies in O^{2-}; however, the catalytic activity of MgO surfaces is attributed to their crystal defects.[17] Just as the results of coordination characterization,

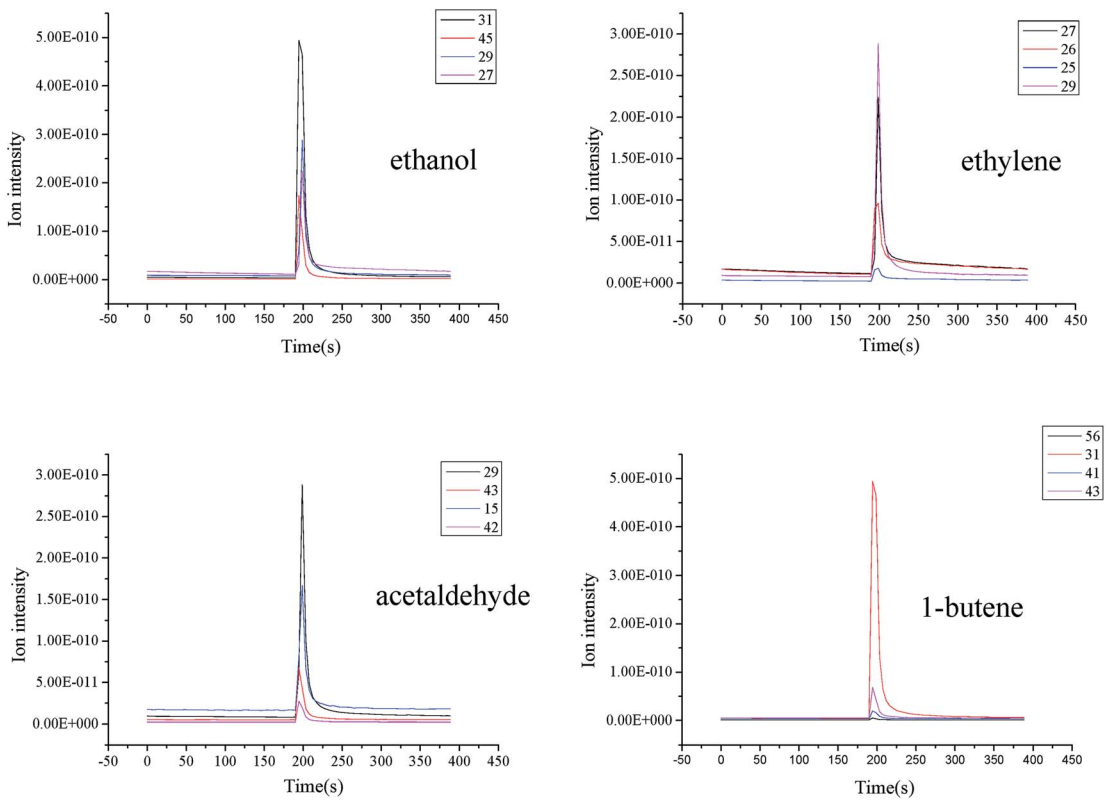

Fig. 3 The ion intensity of products *versus* reaction time on the MgO surface.

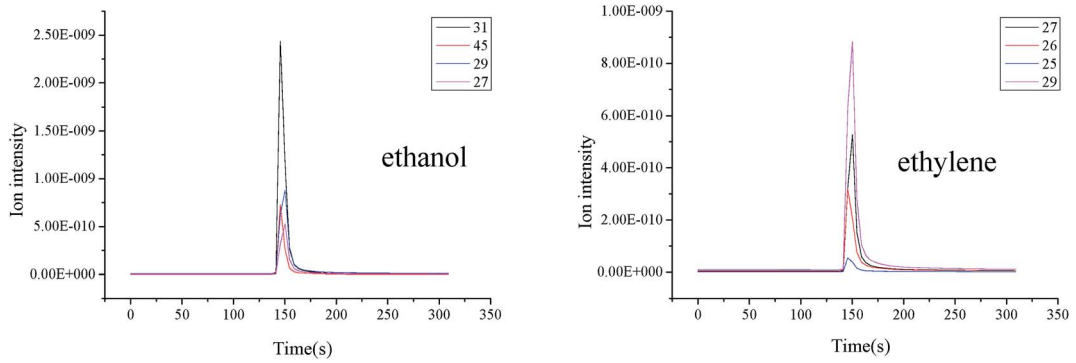

Fig. 4 The ion intensity of products *versus* reaction time on the SiO_2 surface.

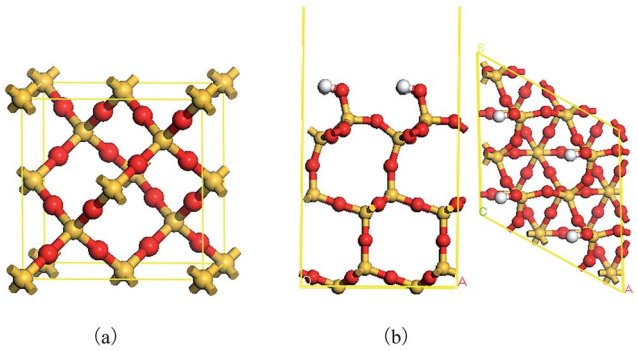

Fig. 5 Crystal models for the SiO_2 surface (a). The model for β-cristobalite; (b). The model for β-cristobalite (111) surface.

the addition of SiO_2 increases the defects of MgO. Thus, the study of reaction species adsorbed on the MgO defects is of great significance. There are three coordination sites of the MgO surface: five-coordinated Mg^{2+} ion at a terrace (Mg5c and O5c), four-coordinated Mg^{2+} ion at a step site (Mg4c and O4c), three-coordinated Mg^{2+} adsorption site at the kink corner (Mg3c and O3c).

In our work, we used the geometry of periclase. The surface energy of MgO (100) is the lowest of; MgO (100), MgO (110), MgO (111)/Mg and MgO (111) by calculations, which agrees with Refson *et al.*[29] Jose A. Rodriguez's work has shown that slabs of 3–4 layers provide a very good representation of the MgO (100) surface.[30] Taking the three types of the above defects into consideration, the model employed in this paper is presented in Fig. 6. The geometry optimization of bulk MgO provides us a typical rock-salt structure with $a_0 = 4.28$ Å, which is close to the experiment measurements (4.22 Å).[31]

3.4 Surface adsorption

3.4.1 The adsorption of ethanol on SiO_2. Taking several adsorption sites and geometry of ethanol on the SiO_2 surface into consideration, the calculation results show that ethanol is adsorbed on a certain site of β-cristobalite (111) and the most stable bonding configurations are shown in Fig. 7. The driving force of ethanol adsorption on the β-cristobalite (111) is that

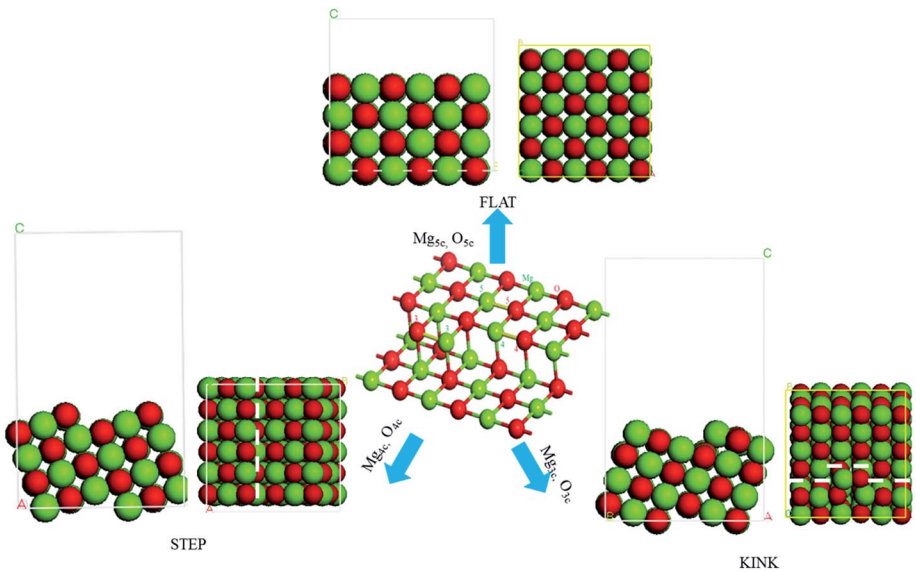

Fig. 6 Optimized geometry diagrams of different MgO surfaces.

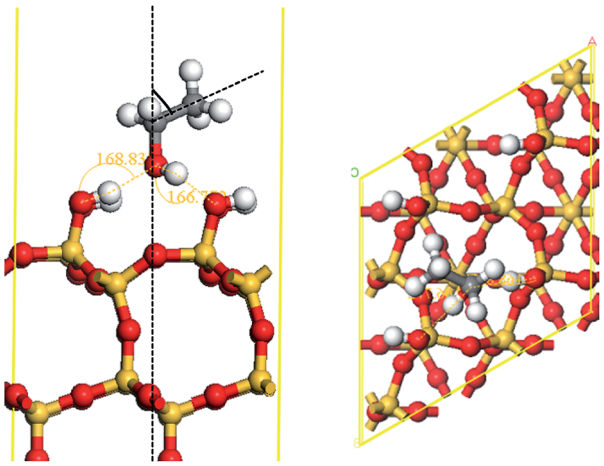

Fig. 7 Stable geometric configurations of CH_3CH_2OH molecule adsorbed on the β-cristobalite (111) surface.

hydrogen bonds are formed between the Si–OH and OH in ethanol. However, the adsorption energy is 0.58 eV, and the adsorption behavior is a weak adsorption.

3.4.2 The adsorption of ethanol on MgO. The stable geometric configurations of ethanol adsorbed on the terrace, step and kink surfaces of MgO are shown in Fig. 8. First, we discuss the stabilities and geometrical parameters of ethanol adsorbed on the terrace sites of MgO, C–C slopes on the surface and the two bonds formed between the ethanol molecule and catalyst surface: H of OH in ethanol with O on the MgO surface (band length = 1.776 Å); O in ethanol with Mg on the MgO surface (band length = 2.352 Å). The adsorption energy is 0.58 eV, which is slightly larger than ethanol on SiO_2.

Dissociative adsorption appears when ethanol is adsorbed on the step sites of MgO, and the adsorption energy is 1.92 eV. The bond length of O–H in ethanol is 2.001 Å, which indicates the cleavage of O–H. The fractured H forms an OH on the flat surface of MgO, and the bond length is 0.985 Å. The O–Mg bond is formed between the Mg5c (bond length = 1.977 Å), Mg4c (bond length = 2.221 Å) and ethoxy group.

Dissociative adsorption also appears when ethanol is adsorbed on the kink sites of MgO, and the adsorption energy is 3.39 eV. The bond length of O–H in ethanol is 4.630 Å, and the fractured H forms an OH with O3c on the kink surface of MgO (bond length = 0.967 Å). The distance between O in ethanol and Mg5c, Mg3c, Mg4c is 2.403 Å, 1.982 Å, 2.131 Å, respectively. Bond length of O–H forming on kink surface of MgO is the shortest, which illustrates that the interaction between ethanol and the kink surface of MgO is the strongest.

In summary, the above results reveal that ethanol is preferably adsorbed on the defective sites of MgO. However, the adsorption of ethanol on MgO or SiO_2 is competitive adsorption, it will produce the by-product of ethylene when ethanol is adsorbed on the SiO_2.[24]

3.4.3 Analysis of density of states. In order to deeply comprehend the interaction between ethanol and SiO_2 or MgO, we also studied density-of-states (DOS) of some relative atoms. For contrast, just the O, H in ethanol and Mg, and O in MgO were selected to calculate DOS. Fig. 9 displays calculated DOS plots for the systems. For ethanol, the O 2p levels are located at 3 to 7 eV and states that it contains a mixture of Mg, while for O in MgO surface and H of OH in ethanol the s character appear between −5 and −9 eV. Furthermore, the overlay area gradually increases and the peak of a strong hybrid appears. This illustrates the interaction between H of OH in ethanol and O on the surface of the catalyst gradually increases from SiO_2, terrace, step to kink.

3.5 Surface reaction

3.5.1 The dehydrogenation of ethanol on flat MgO surface. The adsorption of ethanol on flat MgO has been introduced as part of the adsorption of ethanol on MgO. The initial, transition, and final states of the dehydrogenation of ethanol on the flat MgO surface are shown in Fig. 10. The reaction starts by the H atom moving towards the catalyst surface and the H atom adsorbs at the fcc site (at the TS). The O–H bond distance is elongated to 3.024 Å (at the TS) from the initial 0.982 Å. The reaction barrier is 1.63 eV and the reaction energy is −3.44 eV, indicating a strong exothermic reaction.

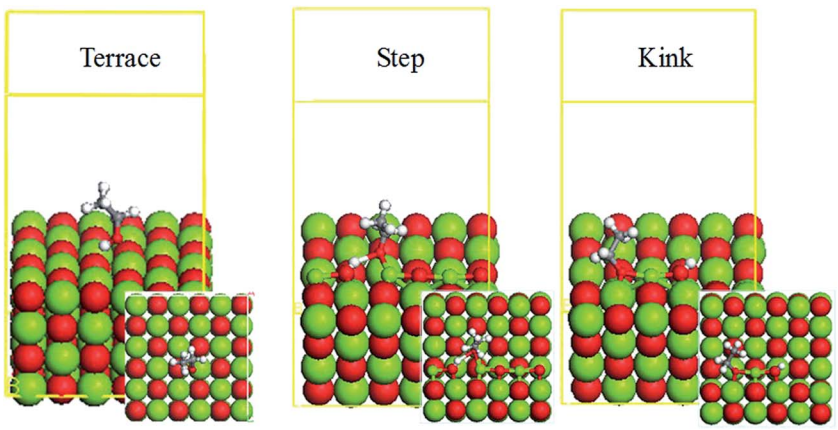

Fig. 8 Stable geometric configurations of the CH_3CH_2OH molecule adsorbed on different MgO surfaces.

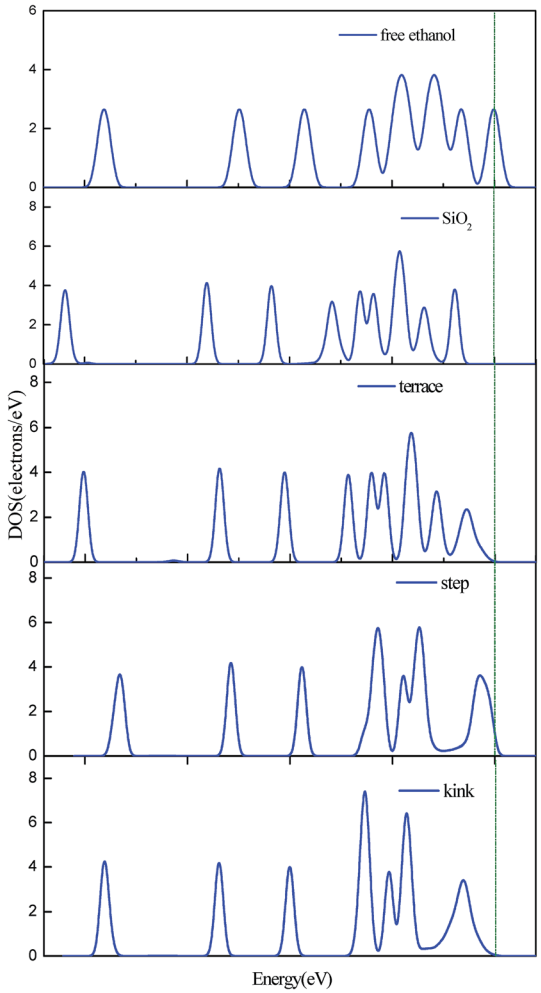

Fig. 9 DOS profiles of the CH_3CH_2OH molecule before and after adsorption on SiO_2 and three different MgO surfaces.

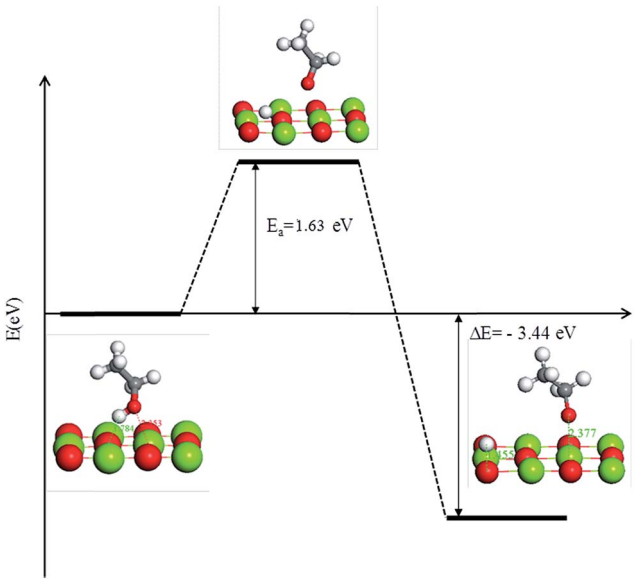

Fig. 10 Potential energy curve for the formation of the ethoxy group from ethanol dehydrogenation on flat MgO surface.

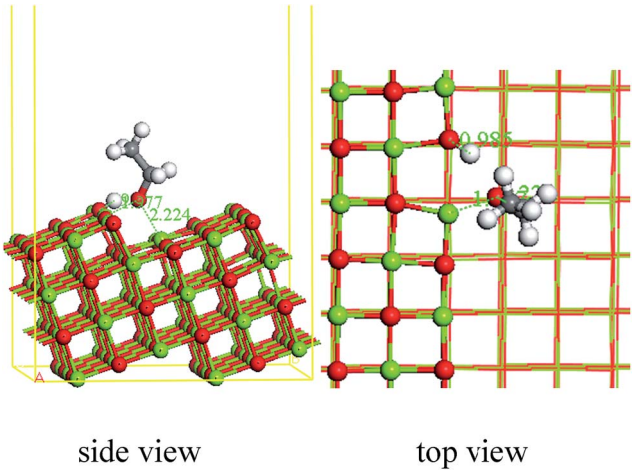

Fig. 11 Stable geometric configuration of the CH_3CH_2OH molecule adsorbed on stepped MgO surface.

3.5.2 The dehydrogenation of ethanol on stepped MgO surface. Dissociative adsorption appeared when ethanol is adsorbed on the stepped sites of MgO, as shown in Fig. 11, and the adsorption energy is 1.92 eV. The bond length of O–H in ethanol is 2.001 Å, which indicates the cleavage of O–H bond. Branda *et al.*[17] investigated the adsorption of ethanol on different defective sites of MgO, and drew the conclusion that dissociative adsorption appeared when ethanol was adsorbed on the low coordination of the MgO surface, whereas there was poor adsorption for flat MgO surface, and our research studies agree with theirs'.

3.5.3 The dehydrogenation of ethanol on kinked MgO surface. Fig. 12 shows that dissociative adsorption also appears when ethanol is adsorbed on the kink sites of MgO, and the adsorption energy is 3.39 eV. The fractured H forms an OH with O3c on the kink surface of MgO (bond length = 0.967 Å). The distance between O in ethanol and Mg5c, Mg3c, Mg4c is 2.403 Å, 1.982 Å, 2.131 Å, respectively.

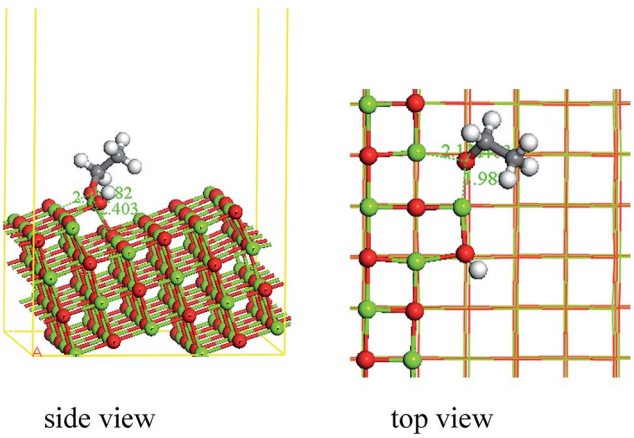

Fig. 12 Stable geometric configuration of the CH_3CH_2OH molecule adsorbed on kinked MgO surface.

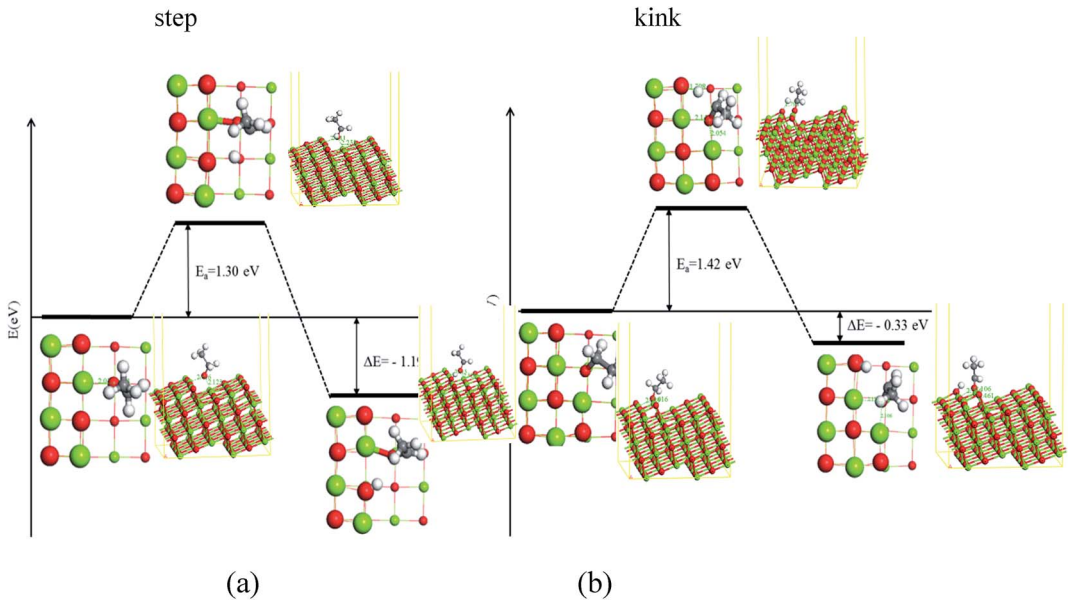

Fig. 13 Potential energy curve for the ethanol dehydrogenation to ethoxy group on stepped and kinked MgO surface.

From the above analysis, we can conclude that the reaction of ethanol to ethoxy group on three surfaces show activity increasing from flat < step < kink, which agrees with the PDOS analysis. Branda *et al.* also draw the conclusion that the adsorption of ethanol on the flat surface is weak and ethanol shows dissociative adsorption on low coordination.[17,32]

3.5.4 The dehydrogenation of ethoxy group on stepped and kinked MgO surface. The above results show that adsorption of ethanol on flat MgO surface is poor, and the activation energy of ethanol dehydrogenation to the ethoxy group is higher, which indicates the dehydrogenation of ethanol to ethoxy group reacts on the defective sites of the MgO surface. Thus, it would be interesting to study the dehydrogenation of the ethoxy group on the step and kink defects of the MgO catalysts and make comparisons with the perfect surfaces studied here.

Fig. 13(a) shows the potential energy curve for the ethanol dehydrogenation to the ethoxy group on stepped MgO surface. The C–H bond is elongated to 2.084 Å at the TS from the initial length of 1.113 Å, while it is further elongated to 2.977 Å in the final state. The distance of H in the ethoxy group to O in stepped MgO surface decreases gradually, until finally reaching 0.997 Å. The reaction barrier is 1.30 eV, and the reaction energy is −1.19 eV, indicating an exothermic reaction.

Fig. 13(b) shows the potential energy curve for the ethanol dehydrogenation to the ethoxy group on kinked MgO surface. The C–H bond is elongated to 1.753 Å at the TS from the initial length of 1.105 Å, while it is further elongated to 1.854 Å in the final state. The distance of H to O, in the ethoxy group on the stepped MgO surface, decreases gradually and finally reaches 0.990 Å. The reaction barrier is 1.42 eV and the reaction energy is −0.33 eV, indicating an exothermic reaction.

4 Conclusions

Through the catalysts characteristics and analysis, we have established models of MgO and SiO_2 surface structures, especially the three defective structures in MgO. The role of SiO_2 in MgO/SiO_2 has been recognised, showing that the structural defects of MgO were increased by adding SiO_2 in the catalyst, which is in favor for the reaction of dehydrogenation of ethanol to acetaldehyde. It provides theoretical guidance for the improvement of catalyst performance in order to enhance the conversion of ethanol to 1,3-butadiene.

The reaction of ethanol dissociation to an ethoxy group was preferable on defective MgO surfaces. The order of adsorption energy of ethanol on three different MgO surfaces is terrace site < step site < kink site. The activation energy for the reaction of ethanol dissociation to an ethoxy group on the flat MgO surface is 1.63 eV, which indicates it is more difficult to react on the flat MgO surface.

The stepped MgO surface is more active for the reaction of dehydrogenation of ethanol to acetaldehyde. The adsorption energy of the ethoxy group on stepped and kinked MgO surface is 1.89 eV and 3.16 eV, respectively. However, the activation energy of dehydrogenation of the ethoxy group to acetaldehyde on stepped MgO surface is 1.30 eV, which is lower than that on the kinked MgO surface (1.42 eV).

Acknowledgements

The authors thank the key laboratory for green chemical technology of ministry of education, for technical assistance.

References

1 W. White, Butadiene production process overview, *Chem.–Biol. Interact.*, 2007, **166**, 10–14.

2 E. V. Makshina, W. Janssens, B. F. Sels and P. A. Jacobs, Catalytic study of the conversion of ethanol into 1,3-butadiene, *Catal. Today*, 2012, **198**, 338–344.
3 Y. Wang and S. J. Liu, Butadiene Production from Ethanol, *J. Bioprocess Eng. Biorefinery*, 2012, **1**, 33–43.
4 K. A. Gray, L. S. Zhao and M. Emptage, Bioethanol, *Curr. Opin. Chem. Biol.*, 2006, **10**, 141–146.
5 B. Hahn-Hagerdal, M. Galbe, M. F. Gorwa-Grauslund, G. Liden and G. Zacchi, Bio-ethanol – the fuel of tomorrow from the residues of today, *Trends Biotechnol.*, 2006, **24**, 549–556.
6 P. Alvira, E. Tomas-Pejo, M. Ballesteros and M. Negro, Pretreatment technologies for an efficient bioethanol production process based on enzymatic hydrolysis: a review, *Bioresour. Technol.*, 2010, **101**, 4851–5486.
7 G. Ezinkwo, V. Tretjakov and R. Talyshinky, Creation of a continuous process for bio-ethanol to butadiene conversion *via* the use of a process initiator, *Catal. Commun.*, 2014, **43**, 207–212.
8 V. L. Sushkevich, I. I. Ivanova, V. V. Ordomsky and E. Taarning, Design of a Metal-Promoted Oxide Catalyst for the Selective Synthesis of Butadiene from Ethanol, *ChemSusChem*, 2014, **7**, 2527–2536.
9 H. J. Chae, T. W. Kim, Y. K. Moon, H. K. Kim, K. E. Jeong, C. U. Kim and S. Y. Jeong, Butadiene production from bioethanol and acetaldehyde over tantalum oxide-supported ordered mesoporous silica catalysts, *Appl. Catal., B*, 2014, **150**, 596–604.
10 B. B. Corson, H. Jones and C. Welling, Butadiene from Ethyl Alcohol: Catalysis in the One-and Two-Stop Processes, *Ind. Eng. Chem.*, 1950, **42**, 359–373.
11 M. Lewandowski, G. S. Babu, M. Vezzoli, M. D. Jones, R. E. Owen and D. Mattia, Investigations into the conversion of ethanol to 1,3-butadiene using MgO: SiO_2 supported catalysts, *Catal. Commun.*, 2014, **49**, 25–28.
12 E. V. Makshina, M. Dusselier, W. Janssens, J. Degrève, P. A. Jacobs and B. F. Sels, Review of old chemistry and new catalytic advances in the on-purpose synthesis of butadiene, *Chem. Soc. Rev.*, 2014, **43**, 7917–7953.
13 S. V. Lebedev, Y. A. Gorin and S. N. Khutoretzkaya, The mechanism of the catalytic conversion of alcohols into biethylene hydrocarbons, *Syntet Kauchuk*, 1935, **4**, 8–27.
14 H. E. Jones, E. E. Stahly and B. B. Corson, Butadiene from Ethyl Alcohol. Catalysis in the One- and Two-Stop Processes, *J. Am. Chem. Soc.*, 1949, **71**, 1822.
15 M. X. Gao, Z. Z. Liu, M. H. Zhang and L. Tong, Study on the Mechanism of Butadiene Formation from Ethanol, *Catal. Lett.*, 2014, **144**, 2071–2079.
16 L. Tong and Z. Z. Liu, Study on catalytic process of 1,3-butadiene from ethanol on MgO/SiO_2 catalyst, *Modern Chemical Industry*, 2012, **32**, 39–42.
17 M. M. Branda, A. H. Rodríguez and P. G. Belelli, Ethanol adsorption on MgO surface with and without defects from a theoretical point of view, *Surf. Sci.*, 2009, **603**, 1093–1098.
18 B. Delley, An all-electron numerical method for solving the local density functional for polyatomic molecules, *J. Chem. Phys.*, 1990, **92**, 508–517.
19 B. Delley, From molecules to solids with the DMol3 approach, *J. Chem. Phys.*, 2000, **113**, 7756–7764.
20 H. J. Monkhorst and J. D. Pack, Special points for Brillouin-zone integrations, *Phys. Rev. B: Condens. Matter Mater. Phys.*, 1976, **13**, 5188.
21 B. Delley, Hardness conserving semilocal pseudopotentials, *Phys. Rev. B: Condens. Matter Mater. Phys.*, 2002, **66**, 155125.
22 J. P. Perdew, K. Burke and M. Ernzerhof, Generalized gradient approximation made simple, *Phys. Rev. Lett.*, 1996, **77**, 3865.
23 S. Coluccia, A. Barton and A. J. Tench, Reactivity of low-coordination sites on the surface of magnesium oxide, *J. Chem. Soc., Faraday Trans. 1*, 1981, **77**, 2203–2207.
24 S. Coluccia, A. J. Tench and R. L. Segall, Surface structure and surface states in magnesium oxide powders, *J. Chem. Soc., Faraday Trans. 1*, 1979, **75**, 1769–1779.
25 D. Jiang and E. A. Carter, First-principles study of the interfacial adhesion between SiO_2 and $MoSi_2$, *Phys. Rev. B: Condens. Matter Mater. Phys.*, 2005, **72**, 165410.
26 D. Ricci and G. Pacchioni, Structure of ultrathin crystalline SiO_2 films on Mo (112), *Phys. Rev. B: Condens. Matter Mater. Phys.*, 2004, **69**, 161307.
27 A. Pelmenschikov, H. Strandh and L. G. Pettersson, Lattice resistance to hydrolysis of Si–O–Si bonds of silicate minerals: *ab initio* calculations of a single water attack onto the (001) and (111) beta-cristobalite surfaces, *J. Phys. Chem. B*, 2000, **104**, 5779–5783.
28 S. Iarlori, D. Ceresoli and M. Bernasconi, Dehydroxylation and silanization of the surfaces of β-cristobalite silica: an *ab initio* simulation, *J. Phys. Chem. B*, 2001, **105**, 8007–8013.
29 K. Refson, R. A. Wogelius, D. G. Fraser, M. C. Payne, M. H. Lee and V. Milman, Water chemisorption and reconstruction of the MgO surface, *Phys. Rev. B: Condens. Matter Mater. Phys.*, 1995, **52**, 10823.
30 J. A. Rodriguez and A. Maiti, Adsorption and decomposition of H_2S on MgO(100), Ni/MgO(100), and ZnO(0001) surface: a first-principles density functional study, *J. Phys. Chem. B*, 2000, **104**, 3630–3638.
31 R. W. G. Wyckoff and R. Wyckoff, *Crystal Structures*, Interscience publishers, New York, 1963, p.102.
32 M. M. Branda, R. M. Ferullo, P. G. Belelli and N. J. Castellani, Methanol Adsorption on Magnesium Oxide Surface with Defects: A DFT Study, *Surf. Sci.*, 2003, **527**, 89–99.

